

# Electro-deoxidation of Ta<sub>2</sub>O<sub>5</sub> in calcium chloride–calcium oxide melts

R. P. Barnett · D. J. Fray

Received: 1 November 2013 / Accepted: 7 February 2014 / Published online: 5 March 2014  
© Springer Science+Business Media New York 2014

**Abstract** Tantalum oxide has been electro-deoxidised in a bath of CaCl<sub>2</sub>-1wt%CaO to form tantalum. It was found that the reaction between the calcium oxide in the melt and the tantalum oxide takes precedence over any reduction process so that until the calcium tantalum oxide Ca<sub>3</sub>(CaTa<sub>2</sub>O<sub>9</sub>) (equivalent to 4CaO·Ta<sub>2</sub>O<sub>5</sub> or Ca<sub>4</sub>Ta<sub>2</sub>O<sub>10</sub>) is formed, calcium ions are reduced to either form calcium metal or reduced calcium species. This eventually results in high electronic conductivity in the melt which means that, compared to the electro-deoxidation of oxides of similar stability to Ta<sub>2</sub>O<sub>5</sub>, the energy and current efficiencies are low. In addition, the vast changes in microstructure result in a structure that is extremely fragile so that the resulting tantalum can only be harvested as a fine powder.

## Introduction

Tantalum has some outstanding properties such as a high melting point, corrosion resistance, and high strength. It is resistant to most acids and bases, with the exception of HF and concentrated fused alkalis, and with these properties it finds applications in the chemical industry. Furthermore, it does not react with body fluids so it can be added to surgical steels. In the field of electronics, it finds extensive use as the capacitor material of choice where tantalum particles

are sintered together, and then oxidised to form a dielectric coating of tantalum pentoxide [1].

Tantalum is prepared from tantalum–niobium oxide ores by dissolving the ores in concentrated HF which is then separated from the niobium by use of methyl isobutyl ketone giving a solution of H<sub>2</sub>TaF<sub>7</sub>. Potassium salts are added to precipitate the tantalum as K<sub>2</sub>TaF<sub>7</sub>. This can be reduced by sodium at elevated temperatures, to give a mixture of KF, NaF and tantalum powder [2].



The potassium fluorotantalate is kept above its melting point of 765 °C. Liquid sodium is added, which floats on the potassium fluorotantalate, to form a mixture of NaF, Na and NaK. The reaction is exothermic causing the melt to be above the boiling point of both Na and K leading to a loss of these two elements. In order to prevent this, the bath is vigorously agitated which serves to drag the sodium into the much denser fluorotantalate phase so that the reaction can proceed with minimal loss of the alkali metals. On completion, the reactor is cooled to ambient temperature and the electrolyte leached away leaving tantalum powder behind. The process is expensive due to the cost of sodium and hazardous due to its high reactivity and problems with the disposal of the fluoride products. Other methods have been explored including electrolysis of the potassium fluorotantalate, hydrogen reduction of tantalum pentachloride or reduction of tantalum pentoxide by carbon at 2000 °C. None of these routes have demonstrated commercial viability. In addition, the oxide route gives a tantalum product with carbon levels far too high for use in capacitors [1, 3].

In the past decade, several new process have been investigated in the laboratory for the reduction of metal oxides. These include electro-deoxidation [4], electronically

R. P. Barnett  
TWI, Granta Park, Great Abington CB21 6AL, UK  
e-mail: roger.barnett@twi.co.uk

D. J. Fray (✉)  
Department of Materials Science and Metallurgy, University of  
Cambridge, Cambridge CB3 0FS, UK  
e-mail: djf25@cam.ac.uk

mediated reaction [5], preform reduction process [6, 7], reduction with calcium [8] and, lastly, a solid oxide membrane process [9]. In the electro-deoxidation process, the metal oxide is made the cathode in a bath of molten calcium chloride–calcium oxide and the favoured cathodic reaction is ionisation of the oxygen which dissolves in the melt, diffuses to the anode then discharged, forming carbon dioxide or oxygen depending on whether a carbon or inert anode is used. The cathode is gradually converted to metal. One of the considerable advantages of this process is the fact that there are very few waste products.

For some metal oxides such as cobalt and nickel oxides the reaction simply consists of the removal of oxygen, leaving the metal behind. For other metal oxides, such as titanium and niobium oxides, the reduction proceeds via calcium compounds and reduced metal oxides. The CaO–Ta<sub>2</sub>O<sub>5</sub> phase diagram contains tantalum oxide, Ta<sub>2</sub>O<sub>5</sub> and calcium tantalum oxides such as CaTa<sub>4</sub>O<sub>11</sub>, CaTa<sub>2</sub>O<sub>6</sub>, Ca<sub>2</sub>Ta<sub>2</sub>O<sub>7</sub>, Ca<sub>4</sub>Ta<sub>2</sub>O<sub>9</sub> and Ca<sub>5</sub>Ta<sub>2</sub>O<sub>10</sub> [10]. Tantalum oxide readily reacts with the electrolyte to form CaTa<sub>4</sub>O<sub>11</sub>, CaTa<sub>2</sub>O<sub>6</sub> and Ca<sub>2</sub>Ta<sub>2</sub>O<sub>7</sub>, all with vastly different morphologies, unlike other metal oxides which do not readily react with the electrolyte without applied cathodic potential. Song et al. [4] have previously examined the electro-deoxidation of Ta<sub>2</sub>O<sub>5</sub>. This paper extends this work and shows that electro-deoxidation is not able to directly reduce Ta<sub>2</sub>O<sub>5</sub> or many of the nCaO·Ta<sub>2</sub>O<sub>5</sub> compounds except 4CaO·Ta<sub>2</sub>O<sub>5</sub>, also written as Ca<sub>3</sub>(CaTa<sub>2</sub>O<sub>9</sub>).

## Experimental procedure

Tantalum pentoxide powder was purchased from PI-KEM then pressed and sintered (1200 °C, 8 h) into porous pellets 20 mm in diameter by 3 mm thick. The pellets had a fairly open structure with a typical grain size of 1–2 μm (as confirmed by scanning electron microscopy), an average open porosity of 28–30 % and an average total porosity of 49 %. All samples (before and after testing) were also sputtered with gold (25 mA for 2 min), prior to examination under scanning electron microscopy, and a 15 kV acceleration voltage was used to take all images and all EDX spectra. All images were taken of the pellet interior; fracture surfaces where the pellet survived intact, powder samples where it did not. This is indicated in the text.

In our previous paper, the drying and preparation procedure for the calcium chloride (thermal drying in a vacuum, followed by addition of 1 wt%CaO) was outlined, although this publication focussed purely on the chemical reaction between the CaCl<sub>2</sub>-1wt%CaO melt and tantalum oxide pellets and not on any reactions occurring under applied potential [11].

The mixed CaCl<sub>2</sub>–CaO was placed in a 310 stainless steel crucible (95 mm internal diameter) and then the

crucible and its contents heated to 850 °C, leading to melting of the CaCl<sub>2</sub>–CaO system. Two graphite rods were then lowered into the melt (to a depth of 40 mm). Using the graphite rods as anode and cathode, the melt was subjected to pre-electrolysis at 1 V for 3 h at 850 °C to remove any remaining redox-active ions, such as Fe<sup>2+</sup>, and moisture. A reproducible background current of 0.19 A was observed after the 3 h regardless of the amount of salt in the crucible. The average total charge passed was 2400 C.

Each pellet of Ta<sub>2</sub>O<sub>5</sub> was mounted in between two sheets of 316 stainless steel mesh (30 × 30 mm, sandwiching the pellet) to prevent any loss of material during the reaction, and then lowered into the melt also to a depth of 40 mm, again, at 850 °C. A potential of 2.7 V was immediately applied between the mesh basket cathode and a graphite anode (separation distance of 55 mm). The pellets were extracted at various points throughout the reaction to analyse the phase and microstructural changes that occurred as the Ta<sub>2</sub>O<sub>5</sub> was reduced to tantalum metal. This was accomplished by allowing the reduction to run for a time before removing the applied potential and extracting the samples from the melt to cool rapidly in the quench zone at the top of the cell, approximately 350 °C cooler than the melt. The mesh cathode was then gently washed in a Soxhlet extractor to remove the remaining salt and then dried gently in a vacuum desiccator. Appropriate pieces of each reduced or partially reduced pellet were then mounted on aluminium stubs for analysis by scanning electron microscopy.

The remainder of each pellet was manually ground and mounted on a holder containing a single silicon crystal cut along the lattice plane. Those samples strong enough to remain intact were mounted as entire pellets if no SEM sample had been extracted. The holder was placed in a Philips Analytical Vertical Diffractometer using Cu Kα radiation. 2 theta values from 10° to 90° were collected and the X-ray diffraction patterns analysed by the use of Highscore™ software. The oxygen and nitrogen contents of the pellets were determined using an Eltra ON900 Simultaneous Oxygen/Nitrogen Determinator. The carbon and sulphur contents were determined using an Eltra CS500 combustion analyser.

## Current curves

The pre-electrolysis current curve provided an immediate indicator of the impurity concentration. With properly dried CaCl<sub>2</sub>, a reproducible pre-electrolysis current of 0.19–0.21 A was observed in the current cell. If the salt was insufficiently dried, this current was less stable, initially presenting as 0.3 A or higher, slowly dropping over 1–2 h to a stable 0.25 A.

Application of a constant voltage of 2.7 V between the basket cathode and the graphite anode led to a varying current flow over time as the  $\text{Ta}_2\text{O}_5$  reacted and was reduced. The difference between the potential to reduce  $\text{Ta}_2\text{O}_5$  and  $\text{CaO}$  to the metal and carbon dioxide is approximately 1 V, so it was believed that the reduction of  $\text{Ta}_2\text{O}_5$  should take preference. This was calculated at 850 °C for Eq. (2), assuming all phases were at unit activity.

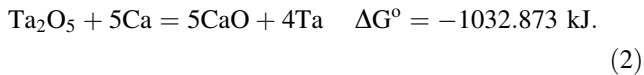


Figure 1 shows a typical plot of the current passed over time, with five distinct features marked.

All five features are reproducible and appeared in almost every electro-deoxidation experiment. The initial current increases very rapidly. As logging began at  $t = 0$ , and the increase took less than 5 s, this increase (Feature A) is not directly visible in Fig. 1 when plotted at this scale. This was followed by a sharp decrease to a local trough (Feature B). The current then shows another increase and subsequent decrease (Feature C) in the 3500–4500 s range. The current then decays at a constant rate (Feature D) before reaching a steady time-invariant current (Feature E). Other oxides, such as  $\text{TiO}_2$ ,  $\text{Nb}_2\text{O}_5$  and  $\text{Cr}_2\text{O}_3$  reduce in a similar way although in some of these cases both the initial current and time-invariant current are lower.

One surprising feature of the current–time curves for  $\text{Ta}_2\text{O}_5$  was the increase in current after approximately 30 min (Features B–C) and the high residual current. Song

et al. [4] found a lower residual current, but the initial current was also lower indicating that more of the applied voltage was lost overcoming the IR loss in the system. After applying potential for 4 h, the calculated current efficiency was only  $\sim 10\%$ ; this was almost entirely due to the high residual current. Residual currents are always observed but as tantalum oxide should reduce at around the same potential as niobium oxide (where the residual currents are much smaller, approx. 0.2 A) this result was somewhat surprising.

### Phases formed during electro-deoxidation

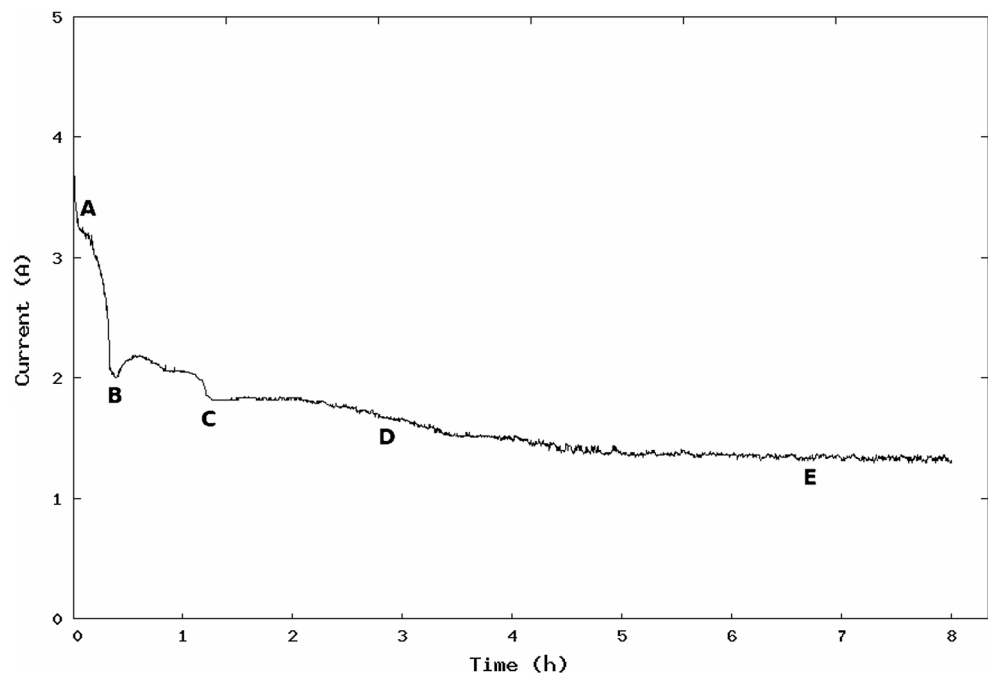
The XRD pattern of the starting  $\text{Ta}_2\text{O}_5$  pellet is shown in Fig. 2.

Figure 3 shows the X-ray diffraction pattern of a pellet which had undergone electro-deoxidation for 0.5 h. No  $\text{Ta}_2\text{O}_5$  was present; the sample consisted entirely of a mixture of three calcium tantalum oxides previously observed to form from chemical interactions with the melt:  $\text{CaTa}_4\text{O}_{11}$ ,  $\text{CaTa}_2\text{O}_6$  and  $\text{Ca}_2\text{Ta}_2\text{O}_7$ . No reduced phases were seen despite the considerable charge that had been passed during this time.

No tantalum metal was observed at this point by X-ray diffraction, or by scanning electron microscopy. The oxygen content (elaborated on later) of these pellets was also greater than that of  $\text{Ta}_2\text{O}_5$ , indicating additional oxygen uptake into the pellet (by formation of calcium tantalum oxides) rather than the removal of oxygen.

After electro-deoxidation for 0.75 h, the sample contained both reduced and unreduced material (Fig. 4).  $\text{Ta}_2\text{O}_5$

**Fig. 1** A typical current–time curve for the reduction of  $\text{Ta}_2\text{O}_5$  in molten  $\text{CaCl}_2$ – $\text{CaO}$  at 850 °C with 2.7 V applied. Typical features are labelled



**Fig. 2** X-ray diffraction pattern of sintered  $\text{Ta}_2\text{O}_5$  pellet prior to reduction

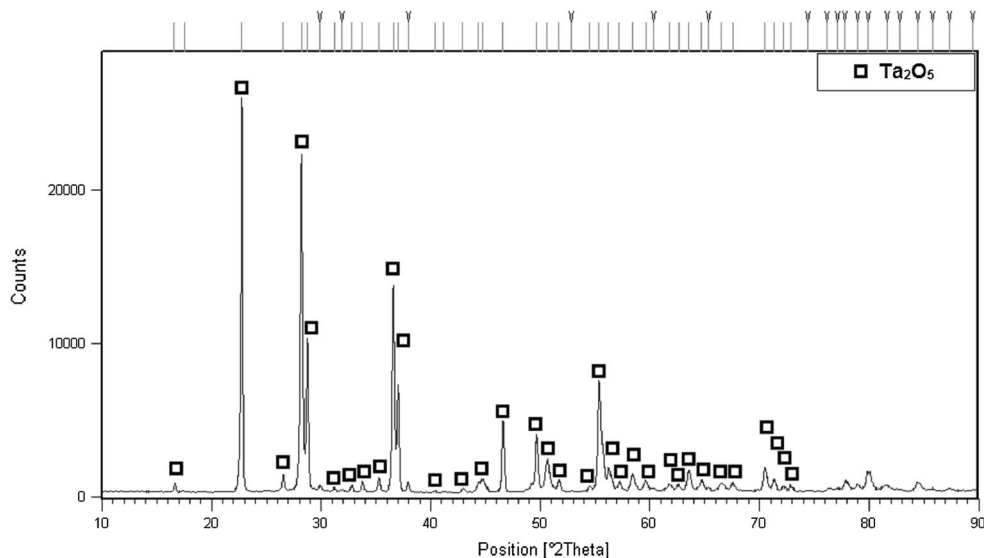
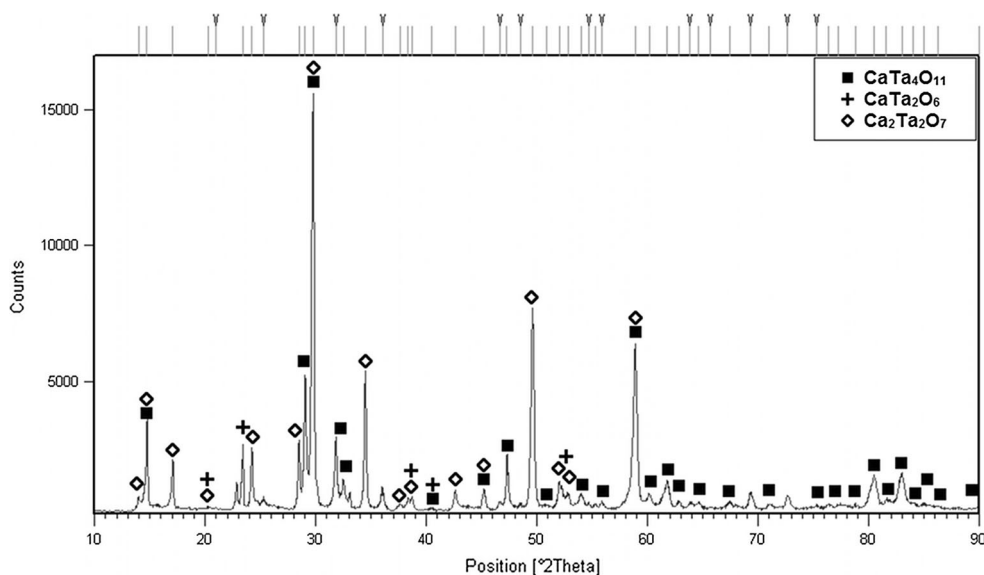


**Fig. 3** X-ray diffraction pattern of a cathode pellet after 0.5 h of reduction in the  $\text{CaCl}_2$ – $\text{CaO}$  melt at 850 °C



and tantalum metal were both present as minor phases.  $\text{CaTa}_2\text{O}_6$  was not present, yet the calcium-rich  $\text{Ca}_2\text{Ta}_2\text{O}_7$  was. The presence of multiple of phases was expected, as the reduction was projected to start on the surface then progress inwards.

After 1–1.5 h, the products were considerably simpler. Only one calcium tantalum oxide  $\text{Ca}_3(\text{CaTa}_2)\text{O}_9$  was present along with tantalum metal. It should be noted that this particular calcium tantalum oxide did not form when samples of  $\text{Ta}_2\text{O}_5$  were submerged in the melt, only when polarisation was applied. The appearance of a shoulder (Feature C) on the current time curves occurred at 1–1.25 h and was believed to correspond to the point at which reduction of calcium tantalum oxides to tantalum metal begins to occur in significant amounts. It is interesting to

note that the current temporarily increases at this point before declining.

Samples extracted after 2, 2.5 and 3 h showed little change in diffraction pattern; the majority of the sample was tantalum metal and the minority was  $\text{Ca}_3(\text{CaTa}_2)\text{O}_9$ . After 4 h of reduction, calcium tantalum oxide was no longer detectable by X-ray diffraction. The only phases present were tantalum and minor tantalum carbide impurities.

Table 1 shows the crystal structures, unit cells and densities (where available) of the phases observed during reduction. Information from the available crystallographic database implied several different crystal structures for each calcium tantalum oxide. Some of these structures appeared to be slightly distorted versions of each other, and

**Fig. 4** X-ray diffraction pattern of a cathode pellet after 0.75 h of reduction in the  $\text{CaCl}_2\text{-CaO}$  melt at 850 °C

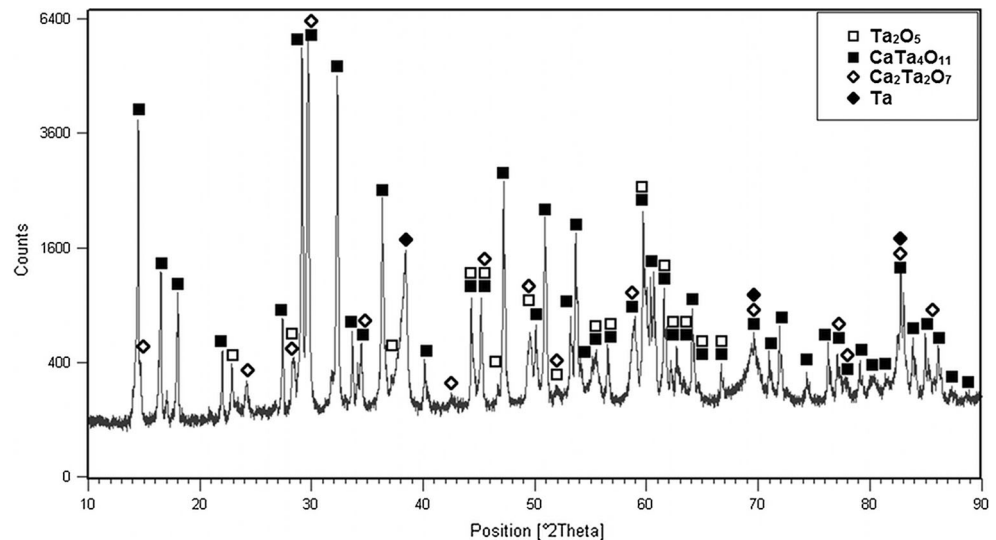


**Table 1** Crystallographic information on  $\text{Ta}_2\text{O}_5$ , Ta and the observed calcium tantalum oxides

Phase (notations are equivalent)	Crystal system	Lattice parameters ( $10^{-10}$ m)	Z	Density ( $\text{g/cm}^3$ )
$\text{Ta}_2\text{O}_5$	Orthorhombic	3.89, 6.21, 44.00	12	8.28
$\text{CaTa}_4\text{O}_{11}$	Hexagonal	6.22, 6.22, 12.27	2	7.6
$\text{CaTa}_2\text{O}_6$	Orthorhombic	5.37, 7.50, 11.07	4	7.4
$\text{Ca}_2\text{Ta}_2\text{O}_7$	Hexagonal	7.36, 7.36, 18.12	6	6.49
$\text{Ca}_3(\text{CaTa}_2)\text{O}_9$	Monoclinic	9.80, 5.53, 7.06	—	—
Ta	Cubic	3.31, 3.31, 3.31	2	16.64

Some information was not available [19]

it was not possible to determine whether this was due to multiple measurements by different laboratories or due to slightly different crystal structures. For the avoidance of ambiguity, Table 1 lists the tantalum oxide, calcium tantalum oxide and tantalum crystal structures which matched the available diffraction patterns. They are listed in the order in which they formed. Additional units of CaO are added to the  $\text{Ta}_2\text{O}_5$  structure sequentially, as the reaction progresses.

The calcium tantalum oxides show a definite trend, becoming less dense with the addition of more CaO to the structure though Ta remains in the (+5) oxidation state. It is also of interest that each transition from one calcium tantalum oxide to the next involves a change in symmetry—alternating from hexagonal to orthorhombic. Comparing the two hexagonal and orthorhombic unit cells (taking the values of Z into account), it was apparent that the unit cell grows as the reaction progresses from start to finish with the structure incorporating the increasing amounts of calcium and oxygen into itself. This structure finally collapses as the  $\text{Ca}_3(\text{CaTa}_2)\text{O}_9$  is reduced to dense cubic tantalum. It is logical to assume that any rearrangement of the atoms in the lattice will take place by the route requiring the least distortion and thus the lowest activation

energy. This may provide explanations for some of the microstructures that were observed.

### Oxygen content

After 0.5 h of passing significant currents, little reduction had occurred. Furthermore, the oxygen content was slightly higher than that of unreduced  $\text{Ta}_2\text{O}_5$  (18.1 wt%) due to the presence of calcium tantalum oxides. These calcium tantalum oxides have a slightly higher oxygen concentration, by weight, than tantalum pentoxide. After 45 min the sample was slightly reduced with an oxygen content (averaged across several samples) of 15.0 wt%.

As seen in Fig. 5 the reduction was initially rapid with the average oxygen content reaching 9.9 wt% after 1 h and 5.5 wt% at 1.5 h. A line of best fit (moving average, period 2) has been added to this figure to show the general trend. The reduction then slowed as the final oxide phases were removed. After 3 h an average of 2.7 wt% oxygen remained, indicating that at least some calcium tantalum oxides were present in the pellet, most likely  $\text{Ca}_3(\text{CaTa}_2)\text{O}_9$  based on information from X-ray diffraction patterns. After 4 h, the sample consisted entirely of

**Fig. 5** Oxygen content of pellets after various reduction times. Values are averaged over several samples with 2–3 oxygen content measurements for each. Measurements of higher oxygen content contain higher errors due to the technique used

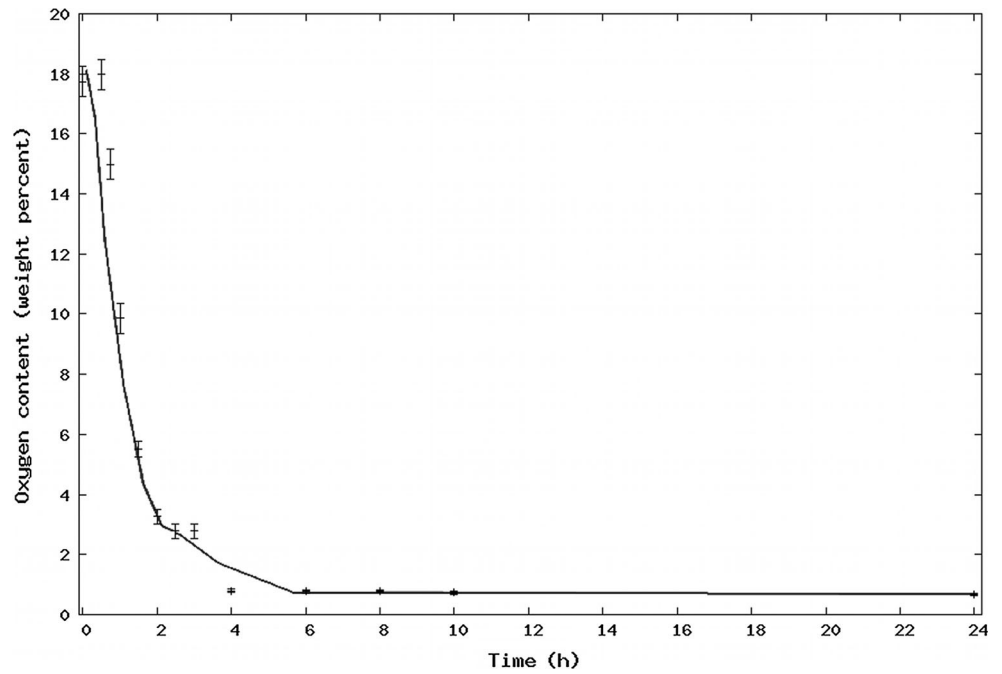
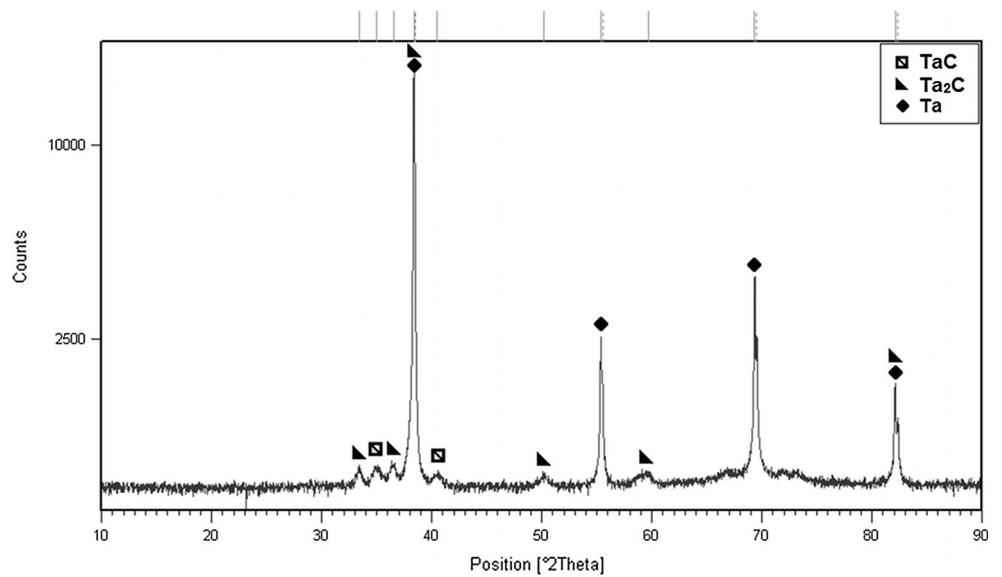


**Fig. 6** X-ray diffraction patterns of pellets reduced for 8 h



tantalum and tantalum carbide impurities with an oxygen content of 0.78 wt% (7800 ppm). No oxide-containing phases were visible on an X-ray diffraction pattern, but oxygen is only soluble in Ta in low concentrations (0.47 % at 1550 °C, falling with temperature). This indicated that the remaining oxygen was present as a combination of Ta–O solid solution, unreduced oxide in quantities too low to be observed by X-ray diffraction and a thin layer of oxide the particle surfaces that formed, when the particles were exposed to air/water. Oxygen removal after 4 h of reduction was slow with the sample still containing 0.73 wt% oxygen after 10 h reduction and 0.67 wt% oxygen after

24 h. This may be due to a shallower concentration gradient.

**Carbide impurities**

Figure 6 shows an X-ray diffraction pattern of a sample (reduced for 8 h) that was heavily carbon contaminated with distinct Ta<sub>2</sub>C peaks, as well as peaks corresponding to TaC. After reduction a black carbon residue remained on the surface of the salt. Upon extraction of the sample, some of this carbon clung to the cathode basket surface, allowing



formation of tantalum carbides through direct reaction between Ta and C outside the melt. The speed of this reaction is not known but could be very high as the reduced tantalum was in the form of a fine powder devoid of a protective oxide film.

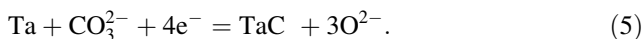
A second carbon source was the formation of carbonate ions ( $\text{CO}_3^{2-}$ ) in the salt either by the dissolution of the liberated  $\text{CO}_2$  in the salt [12],



or by direct reaction at the anode



These carbonate ions could then react directly with the Ta at the cathode to form tantalum carbides



There was no correlation between reduction time and the carbon content, with carbon concentrations in the samples ranging from 600 to 3300 ppm. The average carbon content (taken over a series of partially and fully reduced samples) was 1050 ppm. This was significantly above the carbon concentrations required for capacitor grade powder ( $\sim 100$  ppm or less). Considering the Ta–C phase diagram, at 1500 °C, the solubility of carbon in tantalum is only 0.23 at% [13] and this decreases with temperature [14]. The formation of  $\text{Ta}_2\text{C}$  is feasible at relatively low carbon contents. However, TaC cannot form unless the local carbon concentration is significantly greater ( $>33\%$ ), enough to place the carbon concentration in the two-phase  $\text{Ta}_2\text{C}$ –TaC region. Given that the overall carbon concentrations of the samples are significantly less than this (0.33 % or 3300 ppm), this indicates high local concentrations of carbon, and thus a significant fraction of the carbon was likely present as surface contamination. Modification of the cell design or use of an inert anode would be required to output suitable tantalum. It has been shown that a solid solution of calcium ruthenate in calcium titanate may be suitable as an inert material in these melts [15].

### Microstructural changes

The reduction of  $\text{Ta}_2\text{O}_5$  is characterised by a dramatic series of microstructural changes. The initial stages involve the formation of  $\text{CaTa}_4\text{O}_{11}$  from  $\text{Ta}_2\text{O}_5$  in a similar manner to that observed in chemical reactions between  $\text{Ta}_2\text{O}_5$  and the melt, followed by the formation of  $\text{CaTa}_2\text{O}_6$  and  $\text{Ca}_2\text{Ta}_2\text{O}_7$ . Again, this takes place in a very similar manner to that observed without applied potential. However, the final

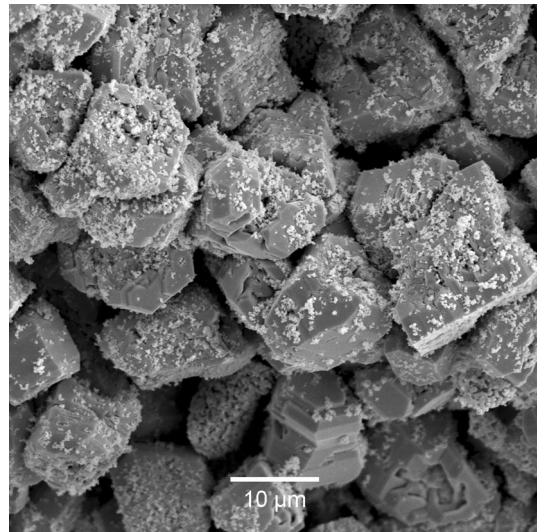
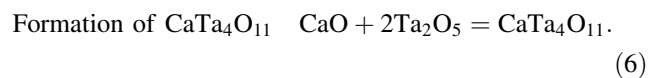


**Fig. 7** SEM micrographs of the initial stage of electro-deoxidation, showing  $\text{CaTa}_4\text{O}_{11}$  encrusted with smaller particles

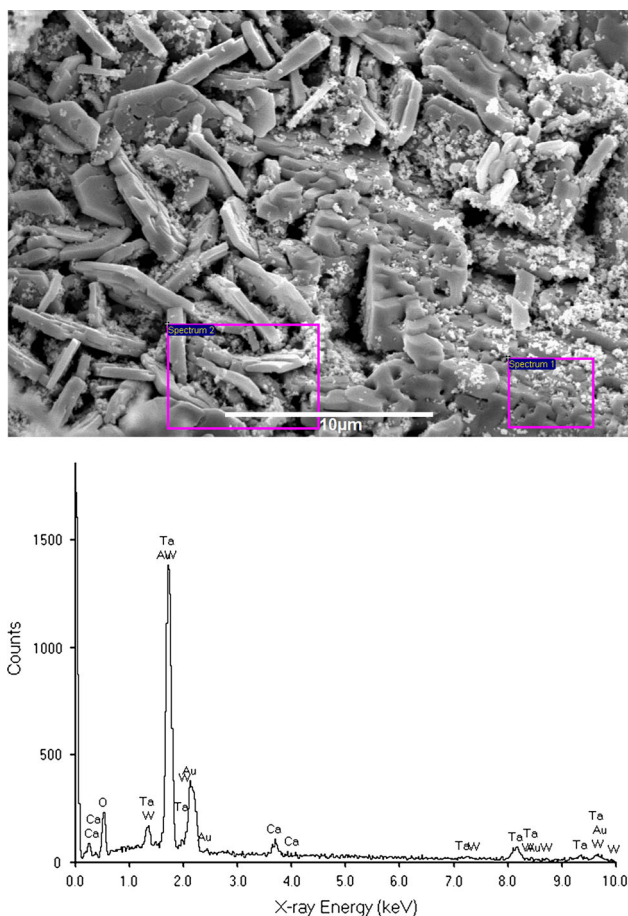
stage differs, with  $\text{Ca}_3(\text{CaTa}_2)\text{O}_9$  forming, followed by tantalum metal. Subsequent reduction involves the removal of oxygen from a primarily tantalum microstructure and leads to no further discernible changes in morphology.

The reaction front progresses through the pellet, beginning at the exterior and continuing inwards. In any one sample, the sample bulk is likely to have progressed less towards the final tantalum metal product than the surface. Multiple stages of reaction may all simultaneously be present in a single sample, though occurring at different positions relative to the pellet exterior. A region in direct proximity is likely to have progressed further along the reaction sequence, given that interaction with the melt is paramount. When the sample has been mostly reduced to tantalum, the remaining  $\text{Ca}_3(\text{CaTa}_2)\text{O}_9$  crystallites are scattered semi-randomly throughout the sample.



Under these conditions  $\text{CaTa}_4\text{O}_{11}$  forms in a similar manner to that observed in the purely chemical reaction between CaO in the melt and  $\text{Ta}_2\text{O}_5$ . However, when a potential is applied, the morphology of this calcium tantalum oxide is significantly different with the formation of much larger particles as shown in Fig. 7. Particles sized 100  $\mu\text{m}$  or greater are observed after only 0.5 h when a potential is applied. In the absence of an applied potential, the particles did not reach this size until at least 4-h exposure. The  $\text{CaTa}_4\text{O}_{11}$  particles are also coated with much smaller encrustations when a potential is applied.

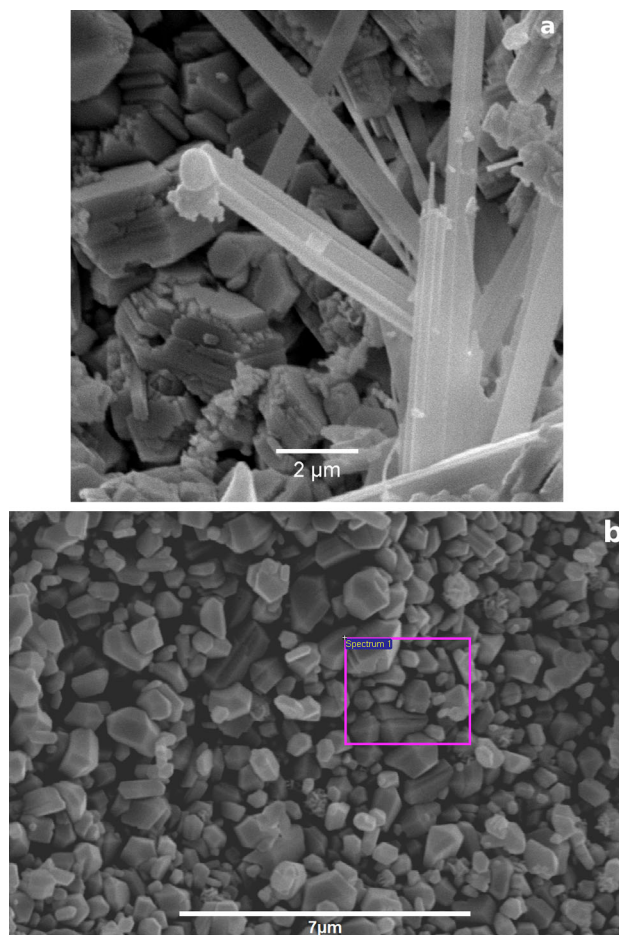
As  $\text{CaTa}_4\text{O}_{11}$  is the only calcium tantalum oxide found in direct proximity to unreduced  $\text{Ta}_2\text{O}_5$  it can be deduced that it forms first, from the starting material. While still possessing a



**Fig. 8** SEM micrograph of  $\text{CaTa}_4\text{O}_{11}$  platelets with corresponding EDX

degree of hexagonal symmetry, the crystallites also do not show the same level of regularity or order as those formed by a purely chemical reaction. They are more rounded, containing more ledges, indicating irregular formation and mismatch.

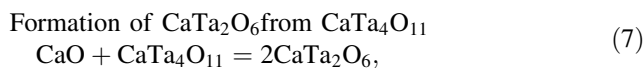
Of considerable interest is that despite the high flow of current in the first 30 min of reduction, no reduced phases can be observed under X-ray diffraction of the samples. These irregular  $\text{CaTa}_4\text{O}_{11}$  particles may provide a partial explanation for this phenomenon. As stated above, this may be that any reduced phases are of small particle size or have low reflectivity, leading to absence from X-ray diffraction spectra. The final tantalum metal has a particle size two orders of magnitude smaller than the observed  $\text{CaTa}_4\text{O}_{11}$  particles. Identification of the encrustations on the  $\text{CaTa}_4\text{O}_{11}$  surface was not possible, due to their smaller size and the fact that they were located only on the surface of  $\text{CaTa}_4\text{O}_{11}$ . EDX showed no elements present besides calcium, tantalum and oxygen, but peaks arising from the  $\text{CaTa}_4\text{O}_{11}$  particles beneath would likely drown out any Ca, Ta or O peaks from the smaller encrustations. At this stage the  $\text{CaTa}_4\text{O}_{11}$  particles are already significantly larger than



**Fig. 9 a** SEM micrograph of  $\text{CaTa}_4\text{O}_{11}$  particles in the process of reacting to form columnar  $\text{CaTa}_2\text{O}_6$ . **b** SEM micrograph of the sample bulk showing mixed calcium tantalum oxides

the starting  $\text{Ta}_2\text{O}_5$  ( $\sim 0.2 \mu\text{m}$ ) and do not attach to their precursor. The  $\text{CaTa}_4\text{O}_{11}$  is less dense than  $\text{Ta}_2\text{O}_5$ , but less porous than its precursor pellet and so does not take up significantly more space. Furthermore, inter-particle joining between different  $\text{CaTa}_4\text{O}_{11}$  crystallites is low, possibly due to the mismatch in crystal symmetries and lattice parameters as shown in Table 1.

This phenomenon leads to the increasing fragility of the sample, even at early stages of reduction. The  $\text{CaTa}_4\text{O}_{11}$  phase is observed almost immediately after reduction begins, and is not fully consumed until the sample has been reduced for an average of 2.5 h. The  $\text{CaTa}_4\text{O}_{11}$  can also be found in the form of hexagonal platelets, showing almost identical EDX results to the more regular crystals but much flatter. These platelets also display eroded edges and faces, likely indicating that these crystals are in the process of reaction, as shown in Fig. 8.





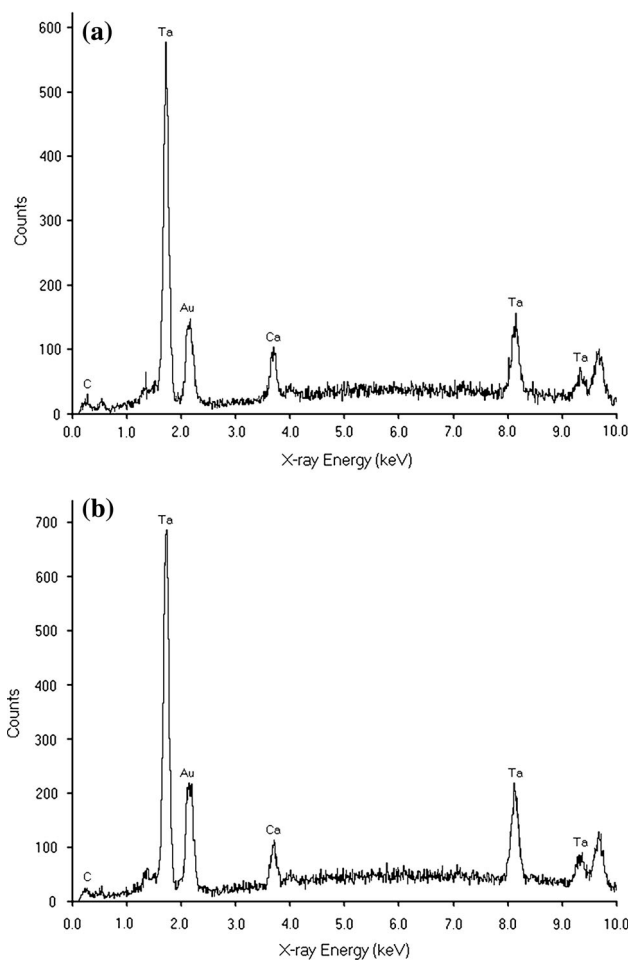
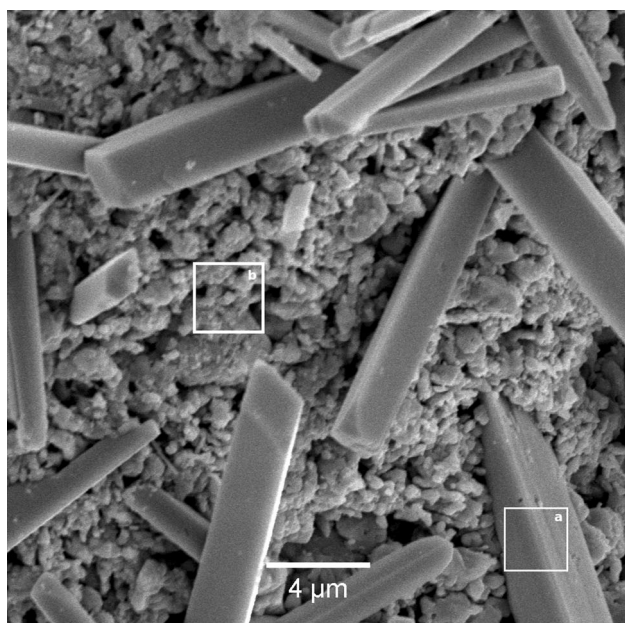
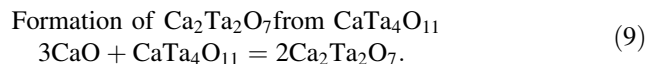
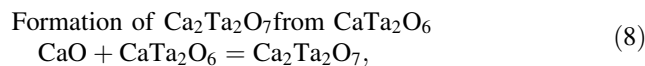


**Fig. 10** SEM micrograph and corresponding EDX spectra of a long columnar calcium tantalum oxide



The middle stages of the reaction are distinguished by two different types of calcium tantalum oxide crystal ( $\text{CaTa}_2\text{O}_6$  and  $\text{Ca}_2\text{Ta}_2\text{O}_7$ ) similar to those produced in a purely chemical reaction (Fig. 9a). The first type are long columns, of the order of  $40 \mu\text{m}$  by  $4 \mu\text{m}$ , the second are needles of a similar length but smaller diameter.

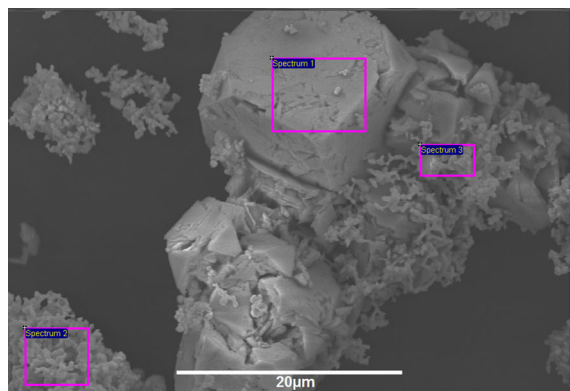
The remainder of the sample (Fig. 9b) can be described as a chaotic series of un-joined small particles ( $\sim 0.5 \mu\text{m}$ ). Some particles have visible facets, others are rounded. From EDX data showing the presence of both calcium and tantalum, as well as its remarkable similarity to the microstructure of samples fully reduced to tantalum, it is believed that this mixture of particles may contain multiple different phases. These include reduced tantalum and small crystallites of various calcium tantalum oxides. The calcium tantalum oxides may come from a variety of sources; they may be dislodged from their nucleation sites, fragmented from larger crystals while said crystals are being reduced, or they may be material in the process of reducing to tantalum metal.

Figure 10 also shows the tips of several long columnar crystals in a sea of mixed crystals. Both the columns and smaller crystals ( $0.5\text{--}1 \mu\text{m}$ ) contain calcium and tantalum with but with more calcium in the smaller crystals. This again likely indicates that the smaller crystals are a mixtures of phases—tantalum and calcium tantalum oxides.

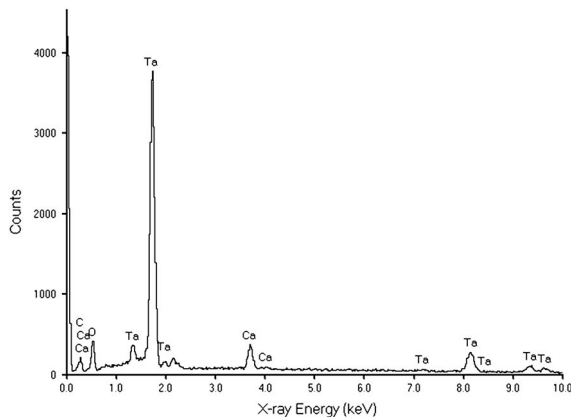
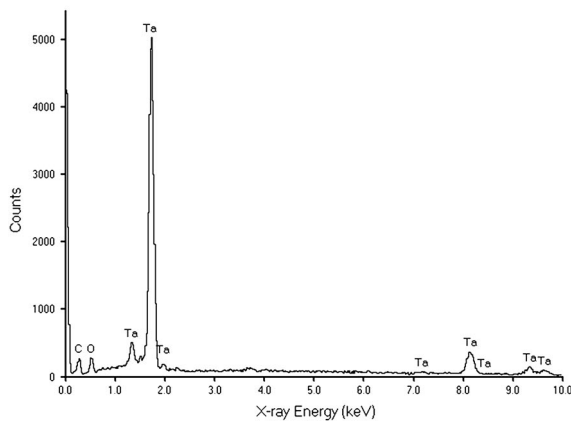
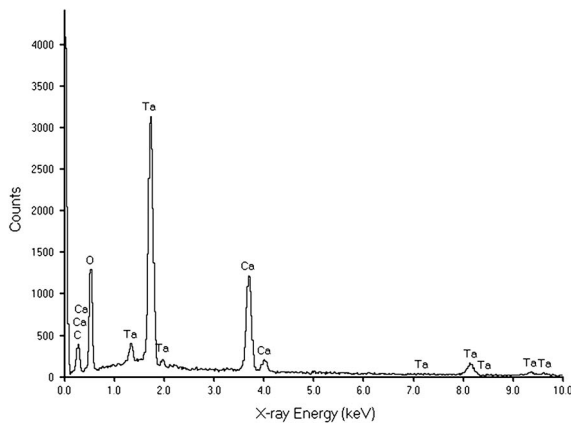
In a previous paper, there was a clear directional preference for the columnar  $\text{CaTa}_2\text{O}_6$  crystals when formed chemically. However, when the pellet was electrochemically reduced, the  $\text{CaTa}_2\text{O}_6$  crystals were found in different arrangements, scattered randomly with no orientation order. The length of the crystals length may be partly due to their crystal structure, with one lattice parameter greater than the others. It was also observed that there was little joining of columns along their edges.

The second distinct crystal type ( $\text{Ca}_2\text{Ta}_2\text{O}_7$  needles) tended to be more common nearer to the surface in partially reduced samples. They require more CaO to form, thus formation is likely more favourable closer to the surface of the sample in direct contact with melt that has not been locally depleted of CaO. Unlike the columnar  $\text{CaTa}_2\text{O}_6$ , these were thinner relative to their length and showed orientation order, even under these conditions of applied potential. They tended to be found in oriented clusters, with their edges joined.

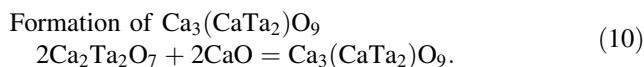
There was evidence of spatial hindrance influencing the growth of both needles and columnar crystals. Both types



◀**Fig. 11** SEM micrograph and corresponding EDX spectra of  $\text{Ca}_3(\text{CaTa}_2)\text{O}_9$  particles in the process of reduction to tantalum metal

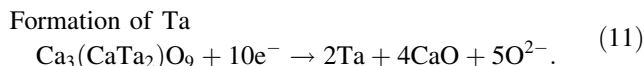


were found throughout partially reduced samples but voids and pores tended to contain a larger fraction of them around the edges. A similar phenomenon was observed on the pellet surface.



After progressing through a chaotic and complex series of calcium tantalum oxides, with different microstructural features, the final stages of the reaction are comparatively simple. The only calcium tantalum oxide present in any quantity discernible by X-ray diffraction is  $\text{Ca}_3(\text{CaTa}_2)\text{O}_9$ , the remainder of the sample is tantalum metal with a small tantalum carbide contamination. The microstructure remains mostly unchanged after this point, even after reduction for 24 h. The  $\text{Ca}_3(\text{CaTa}_2)\text{O}_9$  particles are typically obscured, with tantalum metal grains on the surface. Figure 11 (powder from the centre of a partially reduced pellet, 3 h applied potential) shows a rare example of  $\text{Ca}_3(\text{CaTa}_2)\text{O}_9$  crystallites with the facets and edges clearly visible and only minimal tantalum metal on the surface.

This calcium tantalum oxide appears directly to form tantalum metal when reduced. Considering a sample reduced for 1.5 h with 5.5 wt% oxygen containing only  $\text{Ca}_3(\text{CaTa}_2)\text{O}_9$  and tantalum above the X-ray diffraction detection limit, it can be deduced that the majority of the oxygen present is likely in the form of  $\text{Ca}_3(\text{CaTa}_2)\text{O}_9$ . Samples reduced for longer show only tantalum metal. Therefore, it is probable that the majority of the final tantalum product forms by direct reduction from  $\text{Ca}_3(\text{CaTa}_2)\text{O}_9$ , rather than from other calcium tantalum oxides or from  $\text{Ta}_2\text{O}_5$  directly.



This allows the final stage of the reaction in one region (near-surface) to catalyse earlier stages of the reaction in other regions (pellet interior). The release of four units of CaO per unit of calcium tantalum oxide reduced leads to an increase in local concentration of calcium oxide in the melt. CaO can react with calcium tantalum oxides poorer in CaO (e.g.  $\text{CaTa}_2\text{O}_6$ ) to form those richer in CaO (e.g.  $\text{Ca}_3(\text{CaTa}_2)\text{O}_9$ ). The increased CaO concentration will thus generally increase the rate at which the later calcium tantalum oxides in the reaction series form. The final calcium tantalum oxide  $\text{Ca}_3(\text{CaTa}_2)\text{O}_9$  is then reduced, releasing more calcium oxide in a beneficial loop. As the cathode is not homogeneous, we would expect an accelerated reaction in regions which have form  $\text{Ca}_3(\text{CaTa}_2)\text{O}_9$

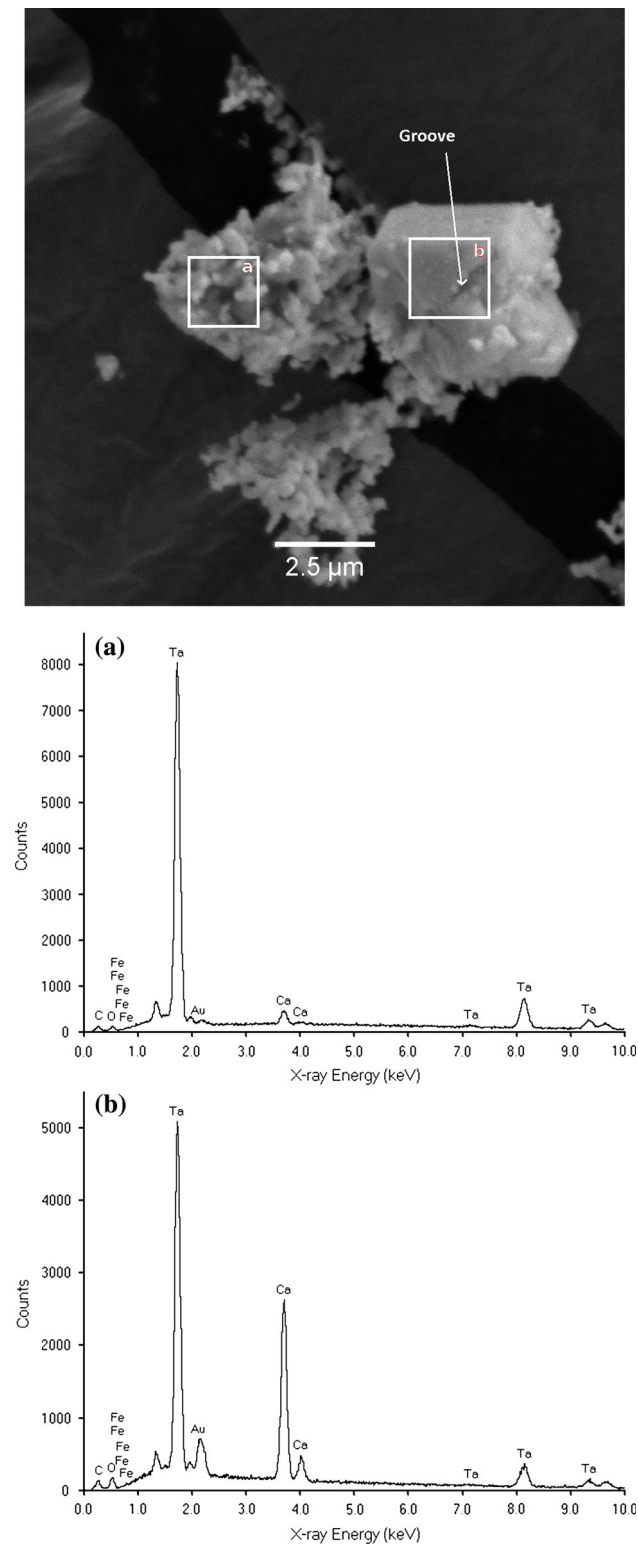


**Fig. 12** SEM micrograph and corresponding EDX spectra of a  $\text{Ca}_3(\text{CaTa}_2)\text{O}_9$  particle in the final stages of reduction to tantalum metal grains

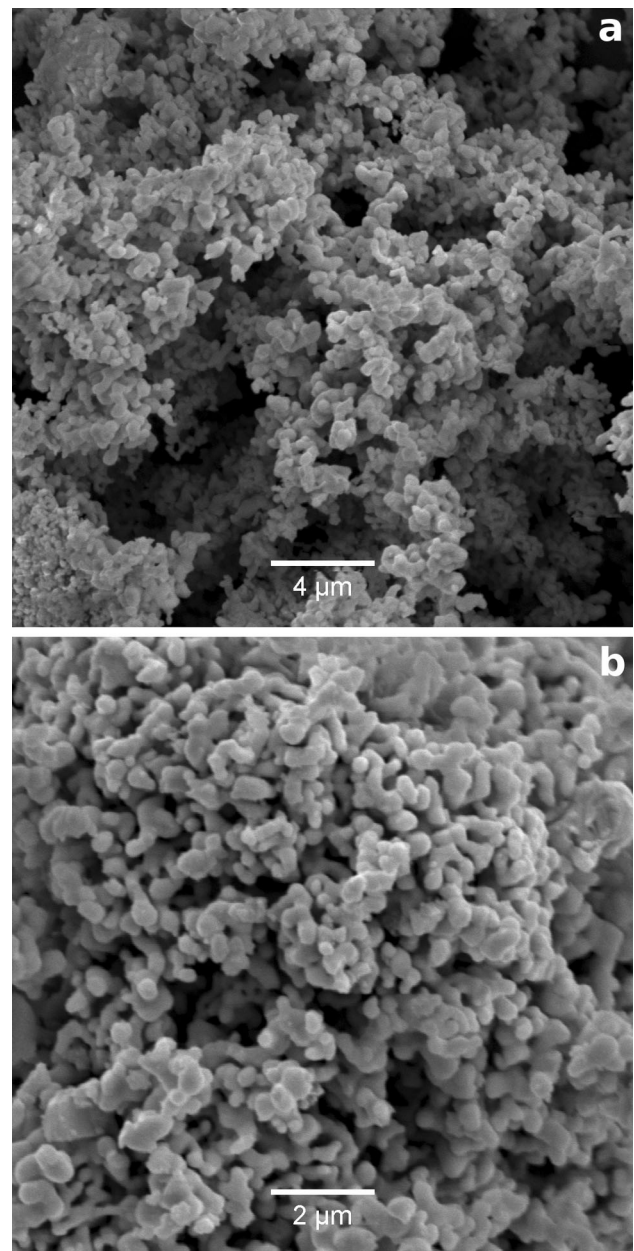


**Fig. 13** Tantalum particles from two samples reduced for **a** 4 h **b** 8 h in molten  $\text{CaCl}_2\text{-CaO}$  at 850 °C with 2.7 V applied

first. Figure 12 (powder from the centre of a partially reduced pellet, 2 h applied potential) shows an example of a  $\text{Ca}_3(\text{CaTa}_2)\text{O}_9$  particle that has almost completely reduced to tantalum metal. It is far more rounded than the previous example, much smaller and displays a groove (labelled) where the reaction may be proceeding, leading to loss of material.

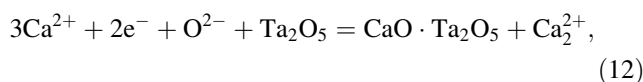


The vast majority of the tantalum present in a fully reduced sample is mostly homogeneous. It consists of rounded particles, 0.1–1  $\mu\text{m}$  in diameter in a nodular structure. On the macroscopic level, the product is fine, black and powdery with little or no mechanical strength after washing, indicating low levels of inter-particle joining. Figure 13 shows two examples of this bulk tantalum microstructure. While no oxygen-containing phases could be discerned, and the oxygen content of these samples was  $>0.78$  wt %, they did contain some tantalum carbide impurities, usually as  $\text{Ta}_2\text{C}$ .

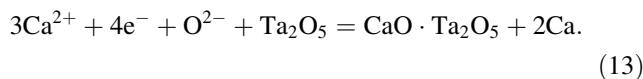
The smaller tantalum particles make up the bulk of the pellet; larger particles are only present near to or on the surface. It perhaps unsurprising that the tantalum particles are so small compared to their predecessor; the density of the tantalum is much higher than  $\text{Ca}_3(\text{CaTa}_2)\text{O}_9$ . A single crystal of this calcium tantalum oxide could not easily collapse in on itself to form a single smaller crystal of tantalum. Formation of smaller tantalum crystals on the surface is more probable, with fragments potentially breaking away due to the lattice mismatch. The microstructure also does not change when the tantalum is reduced using a higher voltage. With all conditions kept the same except the cell voltage (increased from 2.7 to 3.1 V), the microstructure of the reduced tantalum is no different.

### General discussion

Compared to other electro-deoxidation experiments, the results in this work have some very unusual characteristics. The shape of the current time curves is similar to other studies and the reduction involves a series of calcium tantalum oxides. However, no calcium tantalum oxide formation involves an electrochemical reaction, only a chemical reaction with the melt. Electro-deoxidation does not occur until after the  $\text{Ca}_3(\text{CaTa}_2)\text{O}_9$  has formed. No reduced tantalum oxide or calcium tantalum oxide phases form. As there are no electrochemical steps in the first hour of electrolysis involving  $\text{Ta}_2\text{O}_5$  or calcium tantalum oxides, the current must be consumed by other cathodic reactions. There are three possibilities, the first is the deposition of carbon from dissolved carbon dioxide produced at the anode, which is perhaps unlikely at the beginning of the electro-deoxidation, as insufficient  $\text{CO}_2$  is generated. The second is the reduction of  $\text{Ca}^{2+}$  in the melt to form either calcium metal or reduced calcium species in the melt. It seems whilst calcium tantalum oxides are forming, it is easier to reduce calcium ions in the melt rather than to reduce  $\text{Ta}_2\text{O}_5$ .



or

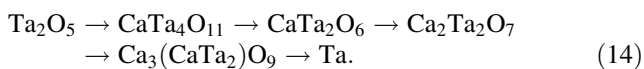


It is known that calcium dissolved in molten calcium chloride can impart electronic conductivity to the melt [16]. A third possibility may be intercalation of calcium into the calcium tantalum oxides, particularly for the hexagonal oxide structures. There is certainly an interaction between the calcium tantalum oxides and calcium; the oxides form more readily and have a slightly different microstructure compared to samples prepared by direct chemical reaction. Furthermore, in order to intercalate calcium, the oxygen activity must be low which increases the electronic conductivity of the pellets [17, 18] which, in turn, increases the volume of active cathode, increasing the rate of reduction. It should be noted that the presence of CaO can lower the conductivity of  $\text{Ta}_2\text{O}_5$ . These potential intercalation compounds may be similar to the lithium intercalation compounds used in lithium-ion batteries. In either case, it is difficult to identify the form of the calcium as the pellets are always washed thoroughly with water. If the calcium were intercalated, this would be released to the melt when the electro-deoxidation of  $\text{Ca}_3(\text{CaTa}_2)\text{O}_9$  to tantalum metal occurred, again increasing the electronic conductivity of the melt (Feature B). This may explain the increase in current during the electro-deoxidation phase. Overall, about 20 % of the charge does not reduce any tantalum compounds. The large residual current during the final removal of oxygen from the solid solution of oxygen in tantalum may be due to the electronic conductivity in the melt. The current efficiency in the tantalum oxide case is about 12 %, whereas for niobium and chromium oxides of similar stability, where similar voltages were applied, the current efficiency is around 80 %. There is similar difference in the energy efficiencies. It is proposed that the energy and current efficiencies be increased by equilibrating the pellets with the electrolyte, so that the calcium tantalum oxides can form by chemical means, prior to applying the potential. In this way, the majority of current would be used for producing tantalum and not calcium which permanently increases the electronic conductivity of the melt. The electronic conductivity can play a major part when the ionic current is controlled by the diffusion of oxygen within the tantalum.

## Conclusions

The first conclusion is that it is possible to form tantalum by electro-deoxidation from a tantalum pentoxide precursor by the FFC-Cambridge process, with low oxygen concentrations (0.79 wt%) after only 4 h of reduction. The primary reaction cell showed low current efficiencies (12 %), but it is believed that this can be increased by preventing the deposition of calcium or reduced calcium species.

The electro-deoxidation of Ta<sub>2</sub>O<sub>5</sub> in molten CaCl<sub>2</sub>–CaO is a complex process, involving multiple steps and the formation of several intermediate calcium tantalum oxides. The overall reaction can be summed up by the following sequential series of reactions:



All of the above except Ta metal can be written in the form  $n\text{CaO}\cdot\text{Ta}_2\text{O}_5$ , where  $n = 0, 0.5, 1, 2$  or  $4$ , with the value of  $n$  increasing throughout the reaction. Curiously, none of the phases observed except the final tantalum metal can be considered reduced; each one contains tantalum in the same oxidation state as Ta<sub>2</sub>O<sub>5</sub>. It is surmised that the current is either being consumed to produce calcium species or for the reduction of the carbonate ion.

The formation of Ca<sub>3</sub>(CaTa<sub>2</sub>)O<sub>9</sub> cannot be purely attributed to a chemical reaction as it does not form when the sample is simply submerged in the melt for a considerable length of time (>24 h). However, it forms in 1 h or less when a cell voltage of 2.7 V is applied, and is completely consumed by the time 4 h have passed, leaving only tantalum metal behind. Once this has reacted, the oxygen present in and on the surface of the tantalum is removed slowly, taking 20 h to go from 0.78 to 0.67 wt%.

Correlating the series of calcium tantalum oxides with the current–time curve, the features present may be assigned to various averaged phase changes. The high initial current falls as the charging reaches its limit, and the reaction front progresses inwards, and is limited by other factors including diffusion. The reproducible current shoulder at 3500–4500 s corresponds to the first appearance of tantalum in the X-ray diffraction pattern, indicating that the tantalum starts forming in considerable quantity at this point. Thus, the current shoulder may be matched to the point at which reduction becomes the significant reaction and calcium is added to the electrolyte. Prior to this, the current is only to reduce calcium ions.

The presence of Ca<sub>3</sub>(CaTa<sub>2</sub>)O<sub>9</sub> and tantalum as the only two phases present after 2–3 h of reduction indicate that the final intermediate phase in many cases is indeed

Ca<sub>3</sub>(CaTa<sub>2</sub>)O<sub>9</sub>, with the majority of the tantalum being formed by direct reduction from this species. However the formation of tantalum from other calcium tantalum oxide phases, or from Ta<sub>2</sub>O<sub>5</sub> directly cannot be ruled out. In all cases, this would increase the local concentration of CaO, speeding the conversion of calcium tantalum oxides to the final Ca<sub>3</sub>(CaTa<sub>2</sub>)O<sub>9</sub> which then reduces to tantalum metal.

**Acknowledgements** The authors are grateful to the EPSRC for financial support and to Metalysis Ltd for financial support, advice and technical support.

## References

- Kock W, Paschen P (1989) Tantalum-processing, properties and applications. *JOM* 41(1):33–39
- Gupta CK (1984) Extractive metallurgy of niobium, tantalum and vanadium. *Int Met Rev* 29(6):405–444
- Hempel CA (1961) Rare metals handbook, 2nd edn. Reinhold Publishing, London
- Song Q-S, Xu Q, Kang X, Du J-H, Xi ZP (2010) Mechanistic insight of electrochemical reduction of Ta<sub>2</sub>O<sub>5</sub> to tantalum in a eutectic CaCl<sub>2</sub>–NaCl molten salt. *J Alloys Compd* 490:241–246
- Okabe TH, Park I, Jacob KT (1999) Production of niobium powder by electronically mediated reaction (EMR) using calcium as a reductant. *J Alloys Compd* 288:200–210
- Yuan B, Okabe TH (2007) Production of fine tantalum powder by preform reduction process using Mg–Ag alloy reductant. *J Alloys Compd* 443:71–80
- Okabe TH, Sato N, Mitsuda Y, Ono S (2003) Production of tantalum powder by magnesiothermic reduction of feed preform. *Mater Trans* 44:2646–2653
- Suzuki RO, Baba M, Ono Y, Yamamoto K (2005) Formation of broccoli-like morphology of tantalum powder. *J Alloys Compd* 389:310–316
- Pal UB, Powell B (2007) The use of solid-oxide-membrane technology for electrometallurgy. *JOM* 59(5):44–49
- Reeve DA (1969) The binary system CaO–Ta<sub>2</sub>O<sub>5</sub>. *J Less Common Met* 17:215–222
- Barnett RP, Fray DJ (2013) Reaction of tantalum oxide with calcium chloride–calcium oxide melts. *J Mater Sci* 48:2581–2589
- Pistorius PC, Fray DJ (2006) Formation of silicon by electro-deoxidation, and implications for titanium metal production. *J S Afr Inst Min Metall* 106:31–41
- Massalski TB, Okamoto H, Subramanian PR, Kacprza L (1990) Binary alloy phase diagrams. ASM, Ohio
- Frisk K, Guillermet AF (1996) Gibbs energy coupling of the phase diagram and thermochemistry in the tantalum–carbon system. *J Alloys Compd* 238:167–179
- Jiao S, Fray DJ (2010) Development of an inert anode for electro-winning in calcium chloride–calcium oxide melts. *Met Mat Trans B* 41:74–79
- Dworkin AS, Bronstein HR, Bredig MA (1961) Ionic melts as solvents for electronic conductors. *Disc Faraday Soc* 32:188–196
- Johannesen O, Kofstad P (1984) The effect of oxide additions on the electrical conductivity of the low temperature form of Ta<sub>2</sub>O<sub>5</sub>. *J Phys Chem Solids* 45(3):239–250
- Johannesen O, Kofstad P (1984) The electrical conductivity of sintered specimens of Ta<sub>2</sub>O<sub>5</sub> with additions of foreign oxides. *Solid State Ionics* 12(3):235–242
- International Centre for Diffraction Data. <http://www.icdd.com>